

1                   **Hornwort pyrenoids: a terrestrial exception with engineering lessons**

2  
3                   Tanner A. Robison<sup>1,2,#</sup>, Juan Carlos Villarreal A.<sup>3,#</sup>, Fay-Wei Li<sup>1,2,4#</sup>, Laura H. Gunn<sup>1,#,\*</sup>

4  
5                   <sup>1</sup>Plant Biology Section, School of Integrative Plant Science, Cornell University, Ithaca, NY,  
6                   USA

7                   <sup>2</sup>Boyce Thompson Institute, Ithaca, NY, USA

8                   <sup>3</sup>Département de Biologie, Université Laval, G1V 0A6, Québec City, QC, Canada

9                   <sup>4</sup>Department of Biology, Duke University, Durham, NC 27710, USA

10  
11                   #Equal contribution

12                   \*Correspondence: lhg42@cornell.edu, ORCID: 0000-0003-2072-0884

13  
14  
15                   **ORCIDiDs**

16                   T.A.R.           0000-0002-1629-9786

17                   J.C.V.A.        0000-0002-0770-1446

18                   F-W.L.         0000-0002-0076-0152

19                   L.H.G.         0000-0003-2072-0884

20  
21                   **Keywords:** *Anthoceros agrestis*, Rubisco, CO<sub>2</sub>-concentrating mechanisms, convergent  
22                   evolution, biomolecular condensates, photosynthesis engineering

## 1 Abstract

2 Ribulose-1,5-bisphosphate carboxylase/oxygenase (Rubisco) underpins nearly all primary  
3 production yet remains a slow, error-prone enzyme because it catalyzes both carboxylation  
4 and oxygenation, the latter initiating photorespiration and reducing net carbon gain. Many  
5 organisms mitigate these limitations not by improving Rubisco selectivity for CO<sub>2</sub> directly,  
6 but by modifying its local environment using CO<sub>2</sub>-concentrating mechanisms (CCMs). In  
7 algae, a prominent biophysical CCM strategy is the pyrenoid: a phase-separated, Rubisco-  
8 rich condensate coupled to bicarbonate transport, local carbonic anhydrase activity, and  
9 diffusion barriers that elevate CO<sub>2</sub> at Rubisco active sites. Although pyrenoids have been  
10 most intensively studied in algal models, a pyrenoid-based CCM has evolved  
11 independently in a single land-plant lineage—the hornworts—providing a powerful  
12 comparative system for understanding how chloroplast organization can be tuned to  
13 terrestrial CO<sub>2</sub>-delivery constraints. Here we synthesize a century of hornwort pyrenoid  
14 research in ecological, phylogenetic, and mechanistic context. We summarize bryophyte  
15 anatomical and microhabitat features that impose strong CO<sub>2</sub> diffusion limitation, and  
16 compare hornwort and algal pyrenoids in ultrastructure, molecular parts lists, and  
17 regulation. We highlight emerging models for hornwort pyrenoid formation, inorganic-  
18 carbon delivery, CO<sub>2</sub> generation and recapture, and recent biochemical/structural work  
19 revealing distinctive hornwort Rubisco properties and biogenesis. Finally, we discuss how  
20 hornwort pyrenoids complement efforts to engineer algal pyrenoid components into C<sub>3</sub>  
21 crops, and propose modular, hybrid engineering strategies that leverage hornwort  
22 compatibility with the embryophyte chloroplast, while selectively importing algal modules.  
23 Together, hornwort pyrenoids illustrate both the convergent logic and the lineage-specific  
24 solutions of biophysical CO<sub>2</sub> concentration, and they open avenues for mechanistic  
25 discovery and photosynthesis engineering.

26

## 27 Introduction

28 Ribulose-1,5-bisphosphate carboxylase/oxygenase (Rubisco) catalyzes the primary step of  
29 carbon fixation and underpins the production of nearly all organic carbon on Earth. Despite  
30 this central role, Rubisco is an unusually poor catalyst: its catalytic turnover is slow, its  
31 affinity for CO<sub>2</sub> is modest, and its active site often fails to discriminate between CO<sub>2</sub> and  
32 O<sub>2</sub>. When O<sub>2</sub> is incorporated instead of CO<sub>2</sub>, Rubisco initiates photorespiration. While  
33 photorespiration is a key plant process linked to a variety of key metabolic processes (for  
34 review see: (Busch, 2020)), excessive photorespiration is metabolically costly and reduces  
35 net carbon gain (for reviews see: (Hagemann and Bauwe, 2016; Walker et al., 2016)).  
36 Across evolutionary history, organisms have adapted to the limitations of this essential and

1 imperfect enzyme in several ways. Many compensate through sheer abundance: in  $C_3$   
2 leaves, Rubisco can account for up to half of all soluble protein (for reviews see: (Whitney  
3 et al., 2011; Prywes et al., 2023)). Others have achieved modest kinetic improvements  
4 through sequence and structural variation ([Bouvier et al. 2024](#)). However, perhaps the most  
5 transformative solutions have not come from altering Rubisco itself, but from modifying the  
6 environment in which Rubisco operates.

7         These environmental strategies are collectively known as  $CO_2$ -concentrating  
8 mechanisms (CCMs). CCMs elevate  $CO_2$  levels around Rubisco, reduce oxygenation  
9 events, and greatly enhance the efficiency of carbon fixation (for reviews see: ([Wunder et](#)  
10 [al. 2019](#); [Liu 2022](#); [Mattinson and Kelly 2025](#); [Monson et al. 2025](#); [Winter and Smith 2022](#))).  
11 They occur in multiple forms depending on lineage and ecology. Biochemical CCMs, such  
12 as  $C_4$  and CAM in vascular plants, rely on metabolic partitioning and specialized leaf  
13 anatomy to increase  $CO_2$  supply. Biophysical CCMs, found in algae and cyanobacteria,  
14 instead use microcompartments, pyrenoids or carboxysomes, that compartmentalize and  
15 co-localize Rubisco with carbonic anhydrases to generate  $CO_2$  directly at the active site.

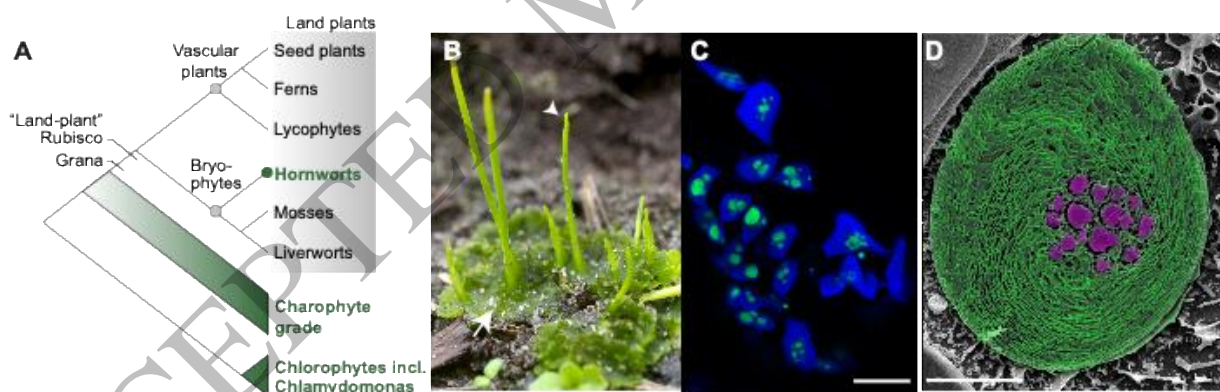
16         Pyrenoids are phase-separated, protein-rich condensates inside the chloroplast  
17 stroma, typically forming a dense Rubisco matrix associated with one or more intrinsically  
18 disordered “linker” proteins ([Barrett et al., 2026](#)). Over the past decade, a surge of work,  
19 driven largely by algal (including diatom) model systems, has transformed pyrenoids from  
20 enigmatic Rubisco-containing “blobs” into tractable molecular assemblies, revealing  
21 principles of condensate organization and motivating ambitious efforts to reconstitute  
22 pyrenoid-like structures in vascular plant chloroplasts ([Hennacy and Jonikas, 2020](#); [Long et](#)  
23 [al., 2025](#); [Barrett et al., 2026](#)).

24         However, pyrenoids are not only an algal innovation. A pyrenoid-based CCM (pCCM)  
25 has evolved in a single lineage of land plants: the hornworts ([Vaughn et al., 1990](#); [Li et al.,](#)  
26 [2017](#); [Robison et al., 2025](#); [Robison et al., 2026](#)). Hornworts are a lineage of bryophytes,  
27 which are non-vascular, seed-free terrestrial plants (Fig. 1A-D). Bryophytes and vascular  
28 plants diverged from each other approximately 500 million years ago, based on molecular  
29 clock estimates ([Morris et al., 2018](#)). This deep evolutionary separation makes hornwort  
30 pyrenoids a powerful comparative system: they likely represent an independent Rubisco  
31 condensation solution, and they have achieved this in a terrestrial context ([Li et al., 2017](#)).  
32 Further, bryophytes have evolved under unique ecological and anatomical photosynthetic  
33 constraints that limit chloroplast  $CO_2$  availability ([Proctor 2000](#)). Thus, the repeated  
34 evolution and retention of a Rubisco condensate is not just a curiosity; it demonstrates  
35 how chloroplast organization can be tuned to terrestrial microenvironments.

1           Hornwort pyrenoids have historically received far less attention than their algal  
 2 counterparts. In this review, we provide a historical perspective of hornwort pyrenoid  
 3 research, discuss constraints on bryophyte photosynthesis, and summarize hornwort  
 4 evolution and phylogeny in the context of pyrenoids. We also compare and contrast algal  
 5 and hornwort pyrenoid molecular composition and ultrastructure, and review the assembly  
 6 and functional divergence exhibited by hornwort Rubiscos. Finally, we discuss how  
 7 hornwort pyrenoids inform current efforts to engineer biophysical CCMs in vascular plants,  
 8 and present outstanding questions and future research opportunities.

9  
 10 Hornwort pyrenoid research: a historical perspective

11 Hornworts are one of the three major bryophyte lineages (together with liverworts and  
 12 mosses) (Nishiyama et al., 2004; Wickett et al., 2014; One Thousand Plant Transcriptomes  
 13 Initiative, 2019; Li et al., 2020) and are the least species rich (Söderström et al., 2016).  
 14 Perhaps because of their deep divergence, hornworts have a perplexing combination of  
 15 traits, including being the only land plant to have pyrenoids (Renzaglia, 1978; Villarreal  
 16 Aguilar and Renzaglia, 2015; Li et al., 2017; Li et al., 2020; Frangedakis et al., 2021).



18  
 19 **Figure 1. Hornworts are the only land plants with pyrenoids.** (A) Phylogeny of major plant groups. Lineages  
 20 that have pyrenoids are colored green. (B) A hornwort plant with sporophytes ( $2n$ ; arrowhead) and  
 21 gametophytes ( $n$ ; arrow) indicated. (C) The model hornwort *Anthoceros agrestis* expressing GFP-tagged  
 22 Rubisco activase (RCA; green), which localizes to pyrenoids and therefore serves as a fluorescent marker for  
 23 pyrenoid position within chloroplasts (blue). Scale bar,  $10\ \mu\text{m}$ . (D) Pseudocolored scanning electron  
 24 microscope image of a hornwort chloroplast (green), showing multiple pyrenoids (purple). Scale bar,  $5\ \mu\text{m}$ .

25  
 26           The first detailed investigations of hornwort pyrenoids came from McAllister in 1914,  
 27 where he described the *Phaeoceros laevis* pyrenoid as a “multiple pyrenoid” consisting of  
 28 dozens to hundreds of small bodies, drawing a clear contrast to the single, spherical

1 bodies found in algae (McAllister, 1914; Lacoste-Royal and Gibbs, 1987; McKay and Gibbs,  
2 1989). Subsequent light microscopic studies would largely confirm these observations  
3 (Scherrer, 1914; Kaja, 1954), although Kaja described the pyrenoid of *Notothylas orbicularis*  
4 as a single body. Despite the structural differences, McAllister hypothesizes (on the basis  
5 of cytological dyes like Millon's Reagent) that the hornwort pyrenoids, like in algae, are  
6 protein rich and are very often surrounded by starch granules. In a later study that included  
7 *N. orbicularis*, McAllister observed that pyrenoids appear to be more clearly defined in  
8 plastids closer to the dorsal surface of the plant, noting a possible association of pyrenoids  
9 with photosynthesis (McAllister, 1927).

10 With the advent of electron microscopy (EM) came new, more detailed  
11 investigations of hornwort pyrenoids. Contrasting with previous reports, these electron  
12 micrographs revealed several pyrenoid units in a chloroplast (Menke, 1961; Manton, 1962;  
13 Sun, 1962; Wilsenach, 1963; Wujek, 1966), rather than dozens or hundreds. This  
14 discrepancy might be explained by artifacts of the staining preparation employed by  
15 McAllister (1914) and Scherrer (1914). Electron microscopy also made clear that individual  
16 pyrenoids were often divided only by tightly appressed thylakoids, but no serial sections  
17 had been performed to determine if pyrenoids are in fact separate or just a highly dissected  
18 structure.

19 These EM investigations, however, focused on *Notothylas*, *Phaeoceros* and  
20 *Anthoceros*, while other genera had been largely ignored and no work had been done on  
21 pyrenoid-lacking hornworts. A more complete survey of hornwort diversity as well as an  
22 attempt to integrate ultrastructural differences in a phylogenetic context was conducted by  
23 Burr (1970). Based on ultrastructural features, Burr arranged species from "primitive"  
24 (algae-like) to "advanced" (vascular plant-like) in a ladder-like fashion (Burr, 1970). Despite  
25 this flawed approach, Burr's detailed ultrastructural investigations revealed the presence  
26 of channel thylakoids, which were previously thought to be artifacts and provided a more  
27 detailed view of hornwort chloroplast ultrastructure. Channel thylakoids are unique to  
28 hornworts: tubular structures running perpendicular to the grana, enriched in photosystem  
29 I, which likely originated from infolding of thylakoid membranes (Burr 1970, Vaughn et al.  
30 1992). Their developmental origin and function in hornwort photosynthetic machinery  
31 remains to be elucidated.

32

33 At the same time, biochemical fractionation and isolation of pyrenoids from the  
34 green alga *Chlamydomonas reinhardtii* (hereafter *Chlamydomonas*) showed strong  
35 enrichment of Rubisco (Holdsworth, 1971; Lacoste-Royal and Gibbs, 1987), helping to  
36 establish the pyrenoid as a central feature of algal carbon fixation and laying the

1 groundwork for its subsequent placement within the CCM framework (Badger and Price,  
2 1992). Building on these insights, Valentine et al. (1986) suggested that hornwort pyrenoids  
3 might likewise contribute to a CCM. Later immunogold labeling revealed that, like observed  
4 in algae, hornwort pyrenoids were indeed the site of Rubisco accumulation (Vaughn et al.,  
5 1990). Vaughn et al. also noted that in the pyrenoid-lacking hornwort species, Rubisco was  
6 dispersed throughout the stroma (Vaughn et al., 1990; Vaughn et al., 1992), suggesting a  
7 lack of a CCM and providing an early comparative framework for testing CCM-related  
8 hypotheses across hornwort lineages.

9         Physiological comparison of the pyrenoid-containing hornwort *Anthoceros*  
10 *punctatus* (*A. crispulus* in the study) to the pyrenoid-lacking liverwort *Pellia endivifolia*  
11 demonstrated that *A. punctatus* has lower carbon isotope discrimination, a lower CO<sub>2</sub>  
12 compensation point, and Ci pool accumulation, which are clear hallmarks of a CCM (Smith  
13 and Griffiths, 1996). Smith and Griffiths also later established that carbonic anhydrase (CA)  
14 inhibitors suppress photosynthesis far more strongly in hornworts than in other bryophytes,  
15 consistent with a CA-dependent CCM that is functionally analogous to biophysical algal  
16 CCMs (Smith and Griffiths, 2000).

17         Comparison of gas exchange characteristics of hornworts with and without  
18 pyrenoids (e.g. *Megaceros*) further revealed that even pyrenoid-lacking hornworts display  
19 weak CCM characteristics, suggesting that the presence of a pyrenoid might strengthen a  
20 CCM, but it is not a prerequisite (Smith and Griffiths, 1996; Hanson et al., 2002). Hanson et  
21 al (2002) also notes that hornworts have additional electron transport requirements  
22 compared to liverworts, especially at low CO<sub>2</sub>, possibly because of additional energy  
23 requirements for the CCM (Burlacot et al., 2022).

24         Over the past century, the somewhat sporadic research into hornwort pyrenoids  
25 clearly established the presence of a biophysical CCM. However, the fundamental  
26 question remains: why did a terrestrial plant lineage evolve a CCM that is otherwise  
27 characteristic of aquatic algae?

28

29 Terrestrialization and the constraints of bryophyte photosynthesis

30 Some 500 million years ago the colonization of land by plants began (Morris et al., 2018).  
31 This course of events radically transformed the composition of the atmosphere, global  
32 nutrient cycles, and the trajectory of life on earth (de Vries and Archibald, 2018). Today, the  
33 near ubiquity of plants on our planet belies the physiological, morphological, and  
34 molecular adaptations required for terrestrialization. Extant land plants can be divided into  
35 two lineages which diverged approximately 450 million years ago: the vascular plants and  
36 the bryophytes (mosses, liverworts, and hornworts) (One Thousand Plant Transcriptomes

1 Initiative, 2019; Li et al., 2020). This deep divergence is reflected in the vast differences in  
2 life cycle, ecological niche, and adaptive traits that these groups evolved to cope with life  
3 ashore. While seed plant adaptations are plainly evident in the sequoias towering over the  
4 forest floor, in the cactus enduring the harsh desert, or the grasses that cover the prairies,  
5 seedless plant adaptations—and bryophytes in particular—are less apparent, leading to  
6 the common misconception that they are “primitive”, “simple”, or “ancient” (Rousk and  
7 Villarreal A, 2025).

8 As plants transitioned to life on land, CO<sub>2</sub>—which diffuses some 10,000 times  
9 slower in water than air—availability to photosynthetic tissue was greatly enhanced, but so  
10 too was the risk of desiccation (Graham et al., 2014). Even today, this tradeoff between  
11 conductance for CO<sub>2</sub> and transpirational water loss is a fundamental constraint of plant  
12 physiology that has guided many of the striking biochemical, structural, and physical  
13 adaptations seen in land plants (Meyer et al., 2008; Clark et al., 2022). In vascular plants,  
14 stomata can respond to environmental cues to balance CO<sub>2</sub> uptake with transpirational  
15 water loss. However, bryophyte gametophytes—the dominant life phase—lack stomata,  
16 precluding such dynamic transpirational regulation (Renzaglia et al. 2017; Pressel et al.  
17 2018). While Fortin and Friedman (2024) proposed that hornwort gametophytic pores could  
18 be homologous to stomata, such pores function as the entry points for symbiotic  
19 cyanobacteria and not for gas exchange (Renzaglia et al., 2009).

20 Bryophytes have largely adapted to minimize transpirational losses at the expense  
21 of their internal conductance for CO<sub>2</sub>, consequently lowering their maximum rate of  
22 photosynthesis (Meyer et al., 2008; Hanson et al., 2014). Even accounting for confounding  
23 factors such as stomata in vascular plants and water films present on the surface of many  
24 bryophytes, conductance for CO<sub>2</sub> is at least an order of magnitude lower in moss leaves  
25 (phyllids) and up to two orders of magnitude lower in thalloid liverworts and hornworts  
26 compared to vascular plants (Meyer et al., 2008). This difference in conductance can be  
27 explained to some extent by the fact that some bryophytes have notably thicker cell walls  
28 than vascular plants (Flexas et al., 2021; Roig-Oliver et al., 2021).

29 In addition to the structural limitations to CO<sub>2</sub> conductance in bryophytes, it is also  
30 worth considering the environments they are best adapted to, and the additional challenge  
31 this presents. Bryophytes often inhabit damp microhabitats where plants are frequently  
32 covered by thin water films following rain, dew, or high humidity, which is crucial for  
33 successful reproduction. Even micron-scale water layers may impose severe diffusional  
34 resistance to CO<sub>2</sub>, slowing gas exchange by orders of magnitude. As a result, bryophytes  
35 periodically experience CO<sub>2</sub> limitation similar to that of aquatic phototrophs. Taken  
36 together, the adaptive and ecological constraints placed on bryophyte carbon fixation are

1 considerable, and these constraints worsen when we view them in the biochemical context  
2 of carbon fixation.

3  
4 Hornworts are uniquely “CCM-ready” among land plants  
5 Why, then, do only hornworts—and no other bryophytes—possess a biophysical CCM? We  
6 speculate that this could be explained by a combination of hornworts’ thallus structure,  
7 monoplastidic nature, and carbon-handling machinery that may have made pyrenoid  
8 evolution comparatively accessible.

9         While mosses and liverworts can certainly experience severe diffusion limitation  
10 when wet, they often mitigate CO<sub>2</sub> delivery constraints (via non-pyrenoid routes),  
11 potentially reducing the selective payoff for a biophysical CCM. For instance, many  
12 complex thalloid liverworts possess air pores and internal air chambers that enhance  
13 internal diffusion (“ventilation” anatomy). Furthermore, mosses and liverworts contain  
14 numerous chloroplasts that are distributed along the cell periphery, maximizing exposure  
15 to incoming CO<sub>2</sub> when it is available. In contrast, many hornworts possess a single large  
16 chloroplast (MacLeod et al., 2022), which has a comparatively low surface area to volume  
17 ratio and may therefore restrict CO<sub>2</sub> delivery. Under these conditions, concentrating CO<sub>2</sub>  
18 around Rubisco may be an adaptation to overcome the limitations of relying on diffusion  
19 alone. Consistent with this idea, hornwort species with multiple epidermal chloroplasts (2–  
20 8 per cell), which would be expected to provide greater chloroplast surface area for gas  
21 exchange, invariably lack pyrenoids (Villarreal and Renner, 2012). This explanation is,  
22 however, not entirely satisfactory as even these multiplastidic hornworts could have a CCM  
23 of some kind, and there are many monoplastidic hornworts that lack pyrenoids (Hanson et  
24 al. 2002; Hanson et al. 2014; Meyer Moritz et al. 2008).

25         However, selection pressure alone is not enough: a functional pyrenoid requires the  
26 existence, and appropriate expression and localization, of the CCM machinery. Just as C<sub>4</sub>  
27 photosynthesis evolved repeatedly by repurposing existing plant genes (Hibberd and  
28 Covshoff, 2010; Emms et al., 2016; Sage, 2016), pyrenoid evolution may be relatively  
29 readily achievable when lineages already possess much of the necessary carbon-handling  
30 toolkit and need only rewire localization and expression. From this perspective, hornworts  
31 may have been effectively ‘CCM-ready’. As we discuss below, hornworts, including  
32 pyrenoid-less species, are the only land plants to have retained orthologs to both of the  
33 chloroplastic carbonic anhydrases (CAH3 and LCIB) that are essential for the  
34 Chlamydomonas CCM, although many mosses and liverworts also have a CAH3 ortholog.  
35 In this context, pyrenoids may be comparatively evolvable in hornworts because their core  
36 innovation is organizational rather than enzymatic: a phase-separated Rubisco matrix can

1 emerge from multivalent binding interactions, and many unrelated proteins could, in  
2 principle, evolve the required linker-like properties.

3

4 Diversity and evolution of hornwort pyrenoids

5 The evolution of pyrenoids in hornworts is notably complex and dynamic. Previous  
6 phylogenetic analyses of one third of all hornwort species and all genera estimated a  
7 Carboniferous crown age for hornworts (and hence potentially for pyrenoids), between 318  
8 and 348 million years ago, coinciding with a precipitous drop in atmospheric CO<sub>2</sub> near the  
9 end of the Devonian period (Peñaloza-Bojacá et al., 2025). As the only plant group inferred  
10 to have diversified under such low atmospheric CO<sub>2</sub>, hornworts may have experienced  
11 selection for successful photosynthesis under these conditions, potentially favoring  
12 pyrenoid evolution. Additional studies have suggested that hornwort pyrenoids have likely  
13 evolved independently multiple times within hornworts in the last 35-50 million years,  
14 coinciding with fluctuating oscillations in atmospheric CO<sub>2</sub>, and that most extant species  
15 diversity is the result of radiation from this period (Villarreal and Renner, 2012). While  
16 pyrenoid-lacking genera *Phaeomegaceros* and *Megaceros* appear to have also diversified  
17 during this period, clades with pyrenoids such as *Anthoceros* and *Dendroceros* tend to be  
18 more species rich.

19 Consistent with recurrent origins, as in C<sub>4</sub> plants, pyrenoid structure and  
20 morphology varies substantially across hornwort lineages. However, the lack of 3D  
21 reconstructions of hornwort chloroplasts limits a full assessment of hornwort pyrenoid  
22 architecture: most studies rely on single-plane EM micrographs (surface views or  
23 transverse sections) from selected tissues, often the gametophyte epidermis. Moreover,  
24 only a handful of taxa have been examined in detail. Based on the available literature  
25 (Vaughn et al., 1992), hornwort pyrenoids can be divided into three main morphological  
26 types. *Anthoceros*-type pyrenoids (*Anthoceros*, including the subgenus *Folioceros*, and  
27 most *Phaeoceros* species) are darkly stained and traversed by multiple thylakoids or even  
28 grana, often giving the appearance of multiple pyrenoid units (Fig 2A). *Notothylas*-type  
29 pyrenoids are typically compact and darkly stained, with a single thylakoid traversing the  
30 matrix. *Dendroceros*-type pyrenoids comprise irregularly shaped subunits and contain  
31 numerous dark inclusions with thylakoids, including short grana, interrupting the pyrenoid.  
32 Channel thylakoids are rarely observed within the pyrenoid matrix, except in lightly-stained  
33 pyrenoids reported for *Nothoceros* and *Phymatoceros* species. Starch grains can  
34 accumulate around the pyrenoid in most species, except *Dendroceros*, especially in  
35 mature plastids but they do not form a solid *Chlamydomonas*-like shell around the  
36 pyrenoid.

1  
2 Structure and organization of hornwort pCCMs  
3 Across eukaryotes, pCCMs share three core functional components: (i) Rubisco, (ii)  
4 compartmentalization of Rubisco into pyrenoids, and (iii) delivery of inorganic carbon  
5 (typically as  $\text{HCO}_3^-$ ) to the vicinity of the pyrenoid, coupled to local conversion of  $\text{HCO}_3^-$  to  
6  $\text{CO}_2$  near Rubisco active sites to create a high- $\text{CO}_2$  microenvironment.

### 8 **The machine: hornwort Rubisco**

9 Rubisco is the central piece of the pCCM. Recently, hornwort Rubisco was found to have  
10 unconventional assembly factor dependencies and kinetic behaviors that depart from  
11 canonical plant Rubisco (Oh et al., 2024). A typical green-type Rubisco is composed of 8  
12 large subunits (RbcL, encoded by the plastid genome) and 8 small subunits (RbcS,  
13 encoded by the nucleus genome). In the green lineage, Rubisco is produced through a  
14 multi-step biogenesis pathway in which general plant chaperonins (Cpn60/Cpn20) and  
15 Rubisco-specific assembly factors (Raf1, Raf2, BSD2, RbcX) shepherd RbcL folding,  $L_8$  core  
16 formation, and RbcS incorporation into the  $L_8S_8$  holoenzyme (Aigner et al., 2017). In  
17 angiosperms, this network is strikingly species-selective, such that “mix-and-match”  
18 assembly across distant lineages often fails, creating a practical bottleneck for both basic  
19 comparative enzymology and Rubisco engineering (Loh and Gunn, 2025).

20 Our recent biochemical and structural work revealed that hornwort Rubisco  
21 biogenesis can markedly diverge from that of other land plants (Oh et al., 2024). Unlike  
22 angiosperm Rubisco, *Anthoceros agrestis* Rubisco assembles efficiently without Raf2 or  
23 RbcX, depending instead only on hornwort-specific combinations of Cpn60 $\alpha/\beta$ , Cpn20,  
24 Raf1, and BSD2. Removing one of the assembly factors, RbcX, essential for assembly of  
25 angiosperm Rubiscos not only failed to disrupt hornwort Rubisco assembly, but increased  
26 catalytic turnover by roughly 50%, implying that hornwort RbcX acts as a structural  
27 modulator rather than an obligate chaperone.

28 Hornwort Rubiscos, including those expressed in the absence of RbcX, exhibit a  
29 range of catalytic turnover rates ( $\sim 3\text{--}10\text{ s}^{-1}$ ), yet show comparatively similar  $\text{CO}_2$  affinity ( $\sim 30$   
30  $\mu\text{M}$ ) and  $\text{CO}_2/\text{O}_2$  specificity ( $\sim 70$ ). This kinetic pattern is notable for two reasons. Firstly,  
31  $\text{CO}_2$  affinity and specificity appear somewhat arbitrarily fixed, regardless of  
32 presence/absence of a CCM. Typically, organisms with CCMs tend to produce Rubiscos  
33 with high catalytic turnover rates, but with reduced specificity consistent with a loosened  
34 selection pressure for high specificity in the high  $\text{CO}_2$  CCM environment (Sage, 2002).  
35 Secondly, the Rubisco literature has historically emphasized a tight inverse coupling  
36 between turnover and specificity (particularly within land plants; (Tcherkez and Farquhar,

1 2021), even if larger modern datasets suggest these correlations may be weaker than  
2 previously assumed (Bouvier et al., 2021). Hornwort Rubiscos thus appear to decouple the  
3 canonical trade-off between catalytic speed and specificity, placing hornwort Rubiscos in a  
4 previously unexplored kinetic space (Oh et al., 2024). Structurally, hornwort Rubisco  
5 resembles other land plant Rubisco enzymes. However, when assembled in the absence of  
6 RbcX, subtle structural differences at the large subunit interfaces loosens the active-site  
7 environment, which could explain the enhanced CO<sub>2</sub>-fixation rates.

8 It should be emphasized that the *A. agrestis* Rubisco synthesized and characterized  
9 by Oh et al (2024) included only one type of RbcS (*AaRbcS1*). As we discuss below, *A.*  
10 *agrestis* harbors another unconventional RbcS isoform that serves as an ‘innate’ Rubisco  
11 linker.

12

### 13 Rubisco condensation

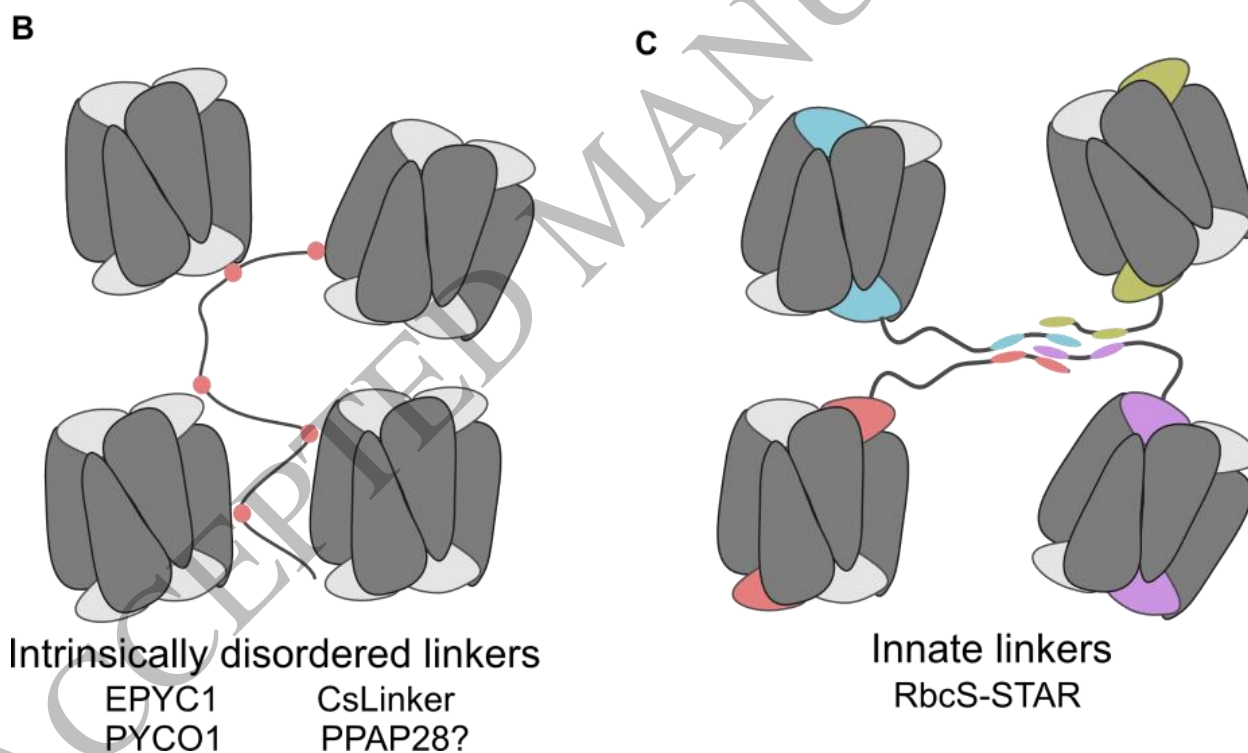
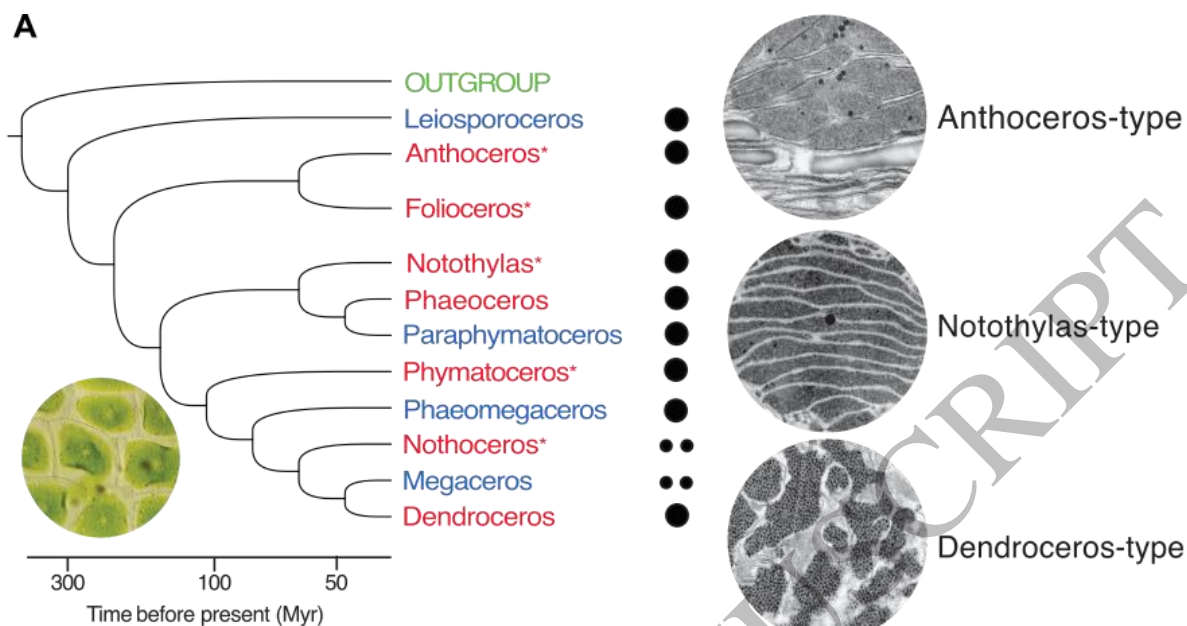
14 Across phylogenetically distant algal lineages, pyrenoid matrices are nucleated by  
15 multivalent “linker” proteins that physically crosslink Rubisco into a dense condensate  
16 (Barrett et al., 2026). Although algal pyrenoid linkers generally lack obvious sequence  
17 similarity (consistent with convergent evolution), these linkers typically follow a sticker-  
18 spacer design: short, repeated “sticker” motifs bind RbcL and/or RbcS, and are separated  
19 by intrinsically disordered spacer regions (Fig. 2B). Because Rubisco presents many  
20 repeated binding sites, a single linker can engage multiple holoenzymes at once,  
21 “crosslinking” Rubiscos into an interaction network. As these weak, multivalent  
22 interactions accumulate, the network demixes from the surrounding stroma to form a  
23 dense condensate. Candidate linkers can often be identified by repetitive motif content,  
24 predicted alternation between locally ordered and disordered segments, and  
25 compositionally biased low-complexity sequences (e.g., regions enriched in  
26 glycine/serine/glutamine/proline and/or charged residues) (Barrett et al., 2024).

27 These linker-Rubisco interactions have now been mechanistically resolved for  
28 several systems. In the diatom *Phaeodactylum tricornutum*, the tandem-repeat/prion-like  
29 protein PYCO1 binds Rubisco via sticker motifs that insert a conserved tryptophan residue  
30 into a phenylalanine-rich hydrophobic cleft on RbcL, stabilized by a small hydrogen-bond  
31 network (Oh et al., 2023). PYCO1 stickers also bind the RbcS ring that lines the central  
32 solvent channel of the Rubisco holoenzyme (at/near the channel entrance), with a key  
33 tryptophan-containing motif contributing to binding. In *Chlamydomonas*, the intrinsically  
34 disordered repeat protein EPYC1 uses multiple short helical stickers to bind RbcS helix  $\alpha$ A  
35 and  $\alpha$ B via salt bridges and a hydrophobic interface (Mackinder et al., 2016; He et al.,  
36 2020). *Chlorella sorokiniana*, from a separate green algal lineage, encodes CsLinker, which  
37 likewise engages Rubisco through electrostatic and hydrophobic contacts. However, unlike

1 EPYC1, CsLinker binds a conserved surface on the RbcL N-terminus rather than RbcS  
2 (Barrett et al., 2024). A candidate linker, PPAP28, has also been reported from the  
3 chlorarachniophyte *Amorphochlora amoebiformis* (Moromizato et al., 2024). PPAP28 is a  
4 largely disordered, repeat-rich pyrenoid-localized protein identified by proteomics, and its  
5 direct role in Rubisco condensation remains to be fully validated.

6 The validated hornwort linker from *A. agrestis* departs sharply from the canonical  
7 algal sticker-spacer arrangement. Here, the linker is a special RbcS bearing an ~100 amino  
8 acid C-terminal extension, termed SequesTration Associated Region (STAR; (Robison et al.,  
9 2026)).

ACCEPTED MANUSCRIPT



1  
2 **Figure 2. Pyrenoid diversity.** (A) Simplified hornwort chronogram with mapped plastid (uni or multiplastidic)  
3 and pyrenoid evolution. Pyrenoid-containing lineages and pyrenoid-lacking lineages are colored red and blue,  
4 respectively. An asterisk (\*) indicates that some species in the genus lack pyrenoids. (B) Depiction of  
5 intrinsically disordered linkers, which have motifs (red circles) that bind to either the Rubisco large or small  
6 subunit. (C) Depiction of RbcS-STAR, an innate linker which is integrated into Rubisco and binds to other  
7 linkers, rather than Rubisco. Rubisco large subunits, canonical RbcS, and RbcS-STAR are shown in dark gray,  
8 light gray, and different colors, respectively.

1  
2 STAR contains three repetitive 23 amino acid motifs (m1, m2, and m3). Compared  
3 with m2 and m3, the m1 sequence shows lower conservation and is predicted to lack  
4 defined secondary structure. Contrastingly, m2 and m3 form coiled coils, displaying  
5 canonical heptad repeats, which are required to produce their distinctive amphipathic  $\alpha$ -  
6 helices. RbcS-STAR is incorporated into the Rubisco holoenzyme in place of a canonical  
7 RbcS, and pyrenoid assembly is driven by coiled-coil interactions between STAR extensions  
8 protruding from neighboring Rubisco, potentially engaging up to four STAR domains. Thus,  
9 unlike algal systems in which condensation is driven primarily by heterotypic linker-  
10 Rubisco interactions, hornwort pyrenoid formation is (thus far) unique in being driven by  
11 self-association of an innate Rubisco linker (Fig. 2C). Notably, while EPYC1 can form  
12 bundled, self-associated assemblies, it does not appear to phase-separate via homotypic  
13 interactions alone; instead, condensation arises primarily through heterotypic EPYC1-  
14 Rubisco crosslinking (Küffner et al., 2024).

15

#### 16 **Possible repeated evolution of RbcS-STAR**

17 Curiously, innate linkers, such as RbcS-STAR, might not be restricted to *A. agrestis*. Similar  
18 RbcS isoforms with a putative C-terminal STAR are also found in *Phaeoceros* species  
19 (Schafran et al., 2025; Robison et al., 2026), which evolved pyrenoids independently  
20 (Villarreal and Renner, 2012). In *Phaeoceros*, these putative innate linkers arose from a  
21 distinct RbcS lineage, and its STAR-like extension shares no detectable sequence  
22 homology with that of *A. agrestis*. Despite this lack of sequence conservation, the  
23 *Phaeoceros* STAR is likewise predicted to form coiled-coil structures, a feature required for  
24 Rubisco condensation in *A. agrestis* (Robison et al., 2026). These observations suggest that  
25 recurrent convergent origins of innate linkers may have underpinned pyrenoid evolution in  
26 hornworts, although functional validation of *Phaeoceros* RbcS-STAR remains necessary.  
27 Conversely, the absence of RbcS-STAR analogs in some pyrenoid-bearing hornworts  
28 indicates that additional distinct mechanisms for Rubisco condensation must exist in  
29 hornworts.

30

#### 31 **Hornwort pyrenoid properties**

32 Pyrenoids differ strikingly in their lifetime and regulatory dynamics. In *Chlamydomonas*,  
33 the pyrenoid matrix behaves as a liquid-like condensate that dissolves and re-condenses  
34 during cell division, and the formation is responsive to environmental cues (Freeman  
35 Rosenzweig et al., 2017; Neofotis et al., 2021; He et al., 2023). This dynamic regulation is

1 achieved through modulating the EPYC1-Rubisco interaction by phosphorylating EPYC1 via  
2 the kinase KEY1 (He et al., 2025). In other algae, classical ultrastructural studies also report  
3 pyrenoid regression or disappearance before division followed by re-formation in daughter  
4 cells (e.g., *Tetracystis excentrica*, *Euglena gracilis*), consistent with cell-cycle-coupled  
5 disassembly/rebuilding in multiple lineages (Brown and Arnott, 1970; Pellegrini, 1980;  
6 Meyer et al., 2017).

7 In contrast, live imaging of *A. agrestis* pyrenoids suggest they are constitutively  
8 present and persist through cell division, with multiple pyrenoids often observed within a  
9 single chloroplast (Lafferty et al., 2024; Robison et al., 2025). Moreover, the hornwort  
10 pCCM has thus far been shown to be constitutive and unresponsive to external CO<sub>2</sub>  
11 concentrations (Hanson et al. 2002; Nötzold et al. 2025). This apparent lack of regulatory  
12 flexibility may stem from the innate nature of the *A. agrestis* linker. Because RbcS-STAR is  
13 an integral component of *A. agrestis* Rubisco, pyrenoid disassembly would require either  
14 turnover of the existing Rubisco pool or a mechanism to weaken, compete with, or actively  
15 remodel the coiled-coil interactions between STAR motifs. Reversible condensates driven  
16 in part by coiled-coil interactions have been demonstrated in both engineered and natural  
17 systems (Ramšak et al. 2023; Yeh et al. 2024; Jiang et al. 2021), indicating that coiled-coil-  
18 mediated matrix assembly is, in principle, compatible with regulated disassembly,  
19 although no such mechanism has yet been identified in hornworts.

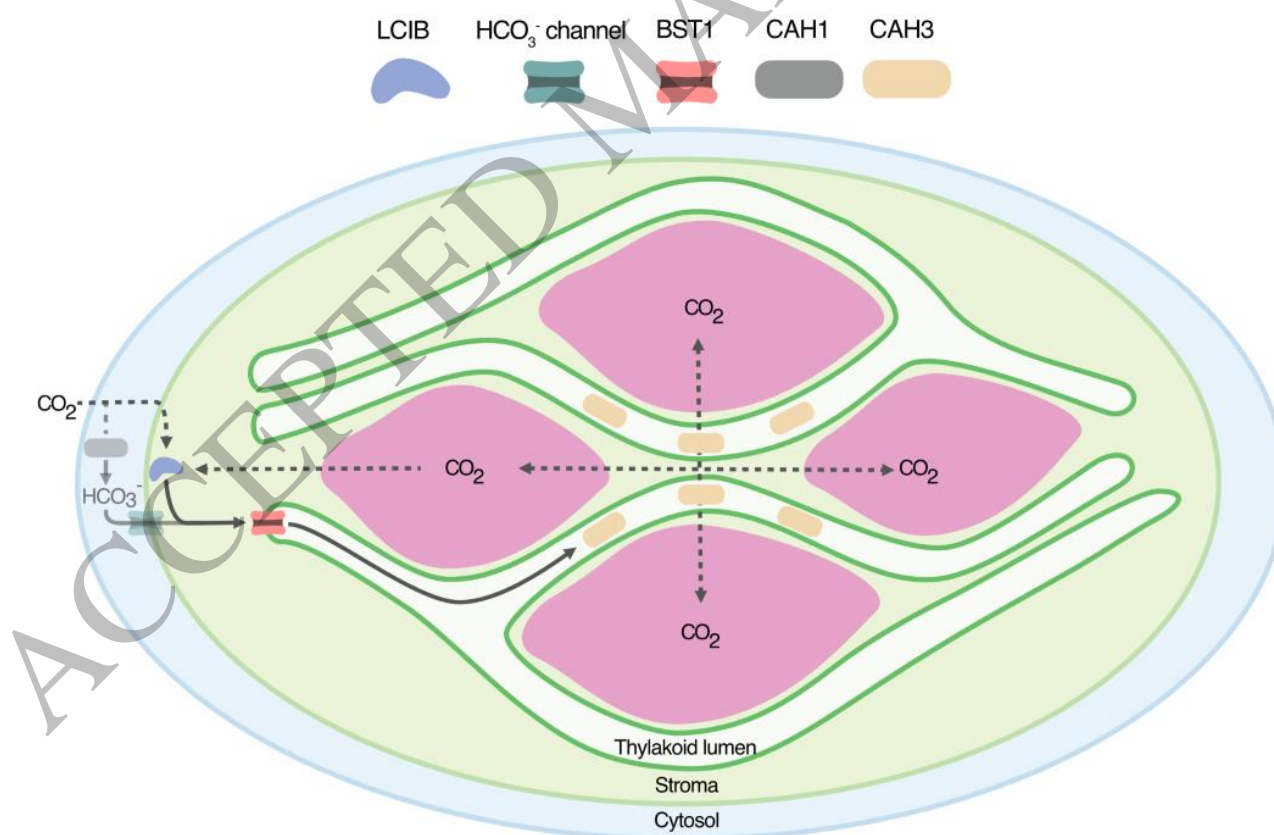
20 Fluorescence recovery after photobleaching (FRAP) experiments indicate different  
21 levels of liquidity depending on which pyrenoid component was targeted (Robison et al.,  
22 2026). Rubisco activase (RCA) recovered quickly after photobleaching, while RbcS-STAR  
23 was relatively immobile. The conventional RbcS isoform, RbcS1, exhibited a range of  
24 mobility, from rapid (like RCA) to slow (like RbcS-STAR). One possible explanation is that  
25 RbcL:RbcS-STAR stoichiometry plays a key role in determining pyrenoid properties.  
26 Fluorescently-tagged RbcS-STAR expression was driven by a strong promoter, and hence  
27 might have artificially increased the ratio of RbcS-STAR to other RbcS isoforms in Rubisco  
28 thereby making the matrix denser. Rubisco stoichiometry heterogeneity could also explain  
29 variability in RbcS1 mobility; because RbcS-STAR occupies the canonical small-subunit  
30 position within the Rubisco holoenzyme, it is competing for that position with RbcS1.  
31 Changing the relative expression of the small subunits, then, may also change the  
32 stoichiometry of RbcL:RbcS-STAR, thus altering the density of the matrix. Since factors like  
33 insert copy number and genomic position can't be controlled in biolistic transformation,  
34 the degree of RbcS1 expression—and therefore mobility—might vary significantly between  
35 transformation events.

36

1 *HCO<sub>3</sub><sup>-</sup> delivery systems*

2 A “Rubisco house” (i.e., a pyrenoid) can, in principle, provide a basal CO<sub>2</sub>-fixation advantage via  
 3 condensation-driven partitioning and mass-action effects (Küffner et al. 2024; Long et al. 2021), but  
 4 robust and efficient CO<sub>2</sub> concentration typically requires additional “plumbing” to accumulate  
 5 inorganic carbon and generate CO<sub>2</sub> near Rubisco. Bicarbonate is transported to the pyrenoid with  
 6 the help of a series of bicarbonate channels. Outside of *Chlamydomonas*, *A. agrestis*, and a  
 7 handful of additional models, bicarbonate delivery to pyrenoids is often supported by physiological  
 8 and comparative evidence rather than molecular pathways. For example, there is evidence of  
 9 bicarbonate acquisition and pumping across chloroplast membranes in haptophytes, but thylakoid  
 10 transport and pyrenoid-proximal CA localization is generally unknown (Nimer and Merrett, 1996;  
 11 Herfort et al., 2002). Similarly, physiological work supports the presence of CCM activity in  
 12 symbiotic dinoflagellates (Leggat et al., 1999; Raven et al., 2020) and in diverse algal groups  
 13 including red algae and cryptophytes (Meyer and Griffiths, 2013), but precise localization and  
 14 molecular details are not yet resolved. *C. sorokiniana* and *A. amoebiformis* currently offer either  
 15 partial localization evidence or proteomic candidate lists rather than a fully resolved pathway  
 16 (Villarejo et al., 1998; Moromizato et al., 2024).

17



18

19 **Figure 3. A spatial model of the pCCM in hornworts.** This schematic summarizes a working model for Ci fluxes  
 20 and CO<sub>2</sub> elevation around condensed Rubisco in *A. agrestis*. Ci is predicted to enter the cytosol and chloroplast  
 21 primarily as CO<sub>2</sub>. BST1 at the thylakoid membrane is hypothesized to mediate HCO<sub>3</sub><sup>-</sup> entry into the thylakoid

1 lumen. LCIB at the chloroplast envelope is proposed to retain stromal  $\text{Ci}$  by trapping incoming  $\text{CO}_2$  and  
2 recapturing  $\text{CO}_2$  that leaks from the pyrenoid region. CAH3 is enriched in specialized, centrally positioned  
3 thylakoids associated with the pyrenoid and is hypothesized to generate  $\text{CO}_2$  near the matrix. The matrix is a  
4 phase-separated, Rubisco enriched compartment (depicted in magenta), and the surrounding thylakoids are  
5 proposed to act as a diffusional barrier. Possible bicarbonate import from the cytosol and into the chloroplast  
6 is depicted with lower opacity vectors to indicate a lack of evidence. Dashed arrows indicate  $\text{CO}_2$  movement;  
7 solid arrows indicate  $\text{HCO}_3^-$  movement.  $\text{Ci}$ , inorganic carbon; LCIB, Low Carbon Inducible protein B; CAH3,  
8 Carbonic Anhydrase 3; BST1, Bestrophin-like channel 1.

9  
10 There is strong evidence in diatoms, including *P. tricornutum*, for a pyrenoid-  
11 associated thylakoid-lumen  $\text{CO}_2$ -generation step but a less unified spatial map (Nakajima  
12 et al., 2013; Kikutani et al., 2016; Raven and Giordano, 2017; Nam et al., 2024).  
13 Nonetheless, many lineages appear to converge on a design in which  $\text{HCO}_3^-$  is  
14 accumulated and then dehydrated to  $\text{CO}_2$  by a pyrenoid-associated, often luminal,  
15 carbonic anhydrase positioned in specialized membranes that traverse or closely contact  
16 the pyrenoid (Sinetova et al., 2012; Kikutani et al., 2016; Young and Hopkinson, 2017; Wang  
17 and Jonikas, 2020; Fei et al., 2022; He et al., 2023).

18 A compartment-resolved inorganic carbon delivery route is best established in  
19 *Chlamydomonas*, and emerging in hornworts (Robison et al., 2025). In *Chlamydomonas*,  
20 bicarbonate channels are located on the plasma (HLA3/LCI1), chloroplast (LCIA) and  
21 thylakoid (BST1) membranes. There is currently limited evidence supporting extracellular  
22 bicarbonate utilization by hornworts. In pH drift experiments, *A. agrestis* reached  
23 equilibrium at slightly higher pH than other bryophytes, but still much lower than aquatic  
24 plants and algae known to utilize bicarbonate, suggesting possible, but weak bicarbonate  
25 utilization in hornworts (Bain and Proctor 1980).  $\text{CO}_2$ , therefore, is likely the dominant  
26 inorganic carbon species entering the cytosol (and potentially the chloroplast), rather than  
27  $\text{HCO}_3^-$ . However, support for intercellular bicarbonate utilization by the hornwort CCM is  
28 more clear. Hornworts accumulate light induced inorganic carbon pools even when the  
29 Calvin-Benson-Bassham Cycle is inhibited and their photosynthesis is greatly reduced  
30 when treated with CA inhibitors (Smith and Griffiths 1996; Smith and Griffiths 2000;  
31 Hanson et al. 2002). Whether hornworts actively import  $\text{HCO}_3^-$  into the chloroplast is  
32 uncertain as hornworts lack a clear LCIA ortholog. Two non-mutually-exclusive entry  
33 scenarios are plausible: (i)  $\text{CO}_2$  diffuses into the cytosol, is converted to  $\text{HCO}_3^-$  by a  
34 cytosolic carbonic anhydrase, and  $\text{HCO}_3^-$  is then imported across the chloroplast envelope  
35 by as-yet-unidentified transporters; and/or (ii)  $\text{CO}_2$  diffuses across the chloroplast  
36 envelope and is converted to  $\text{HCO}_3^-$  in the stroma by the hornwort LCIB ortholog (Fig. 3).

1           Once bicarbonate has been delivered to the pyrenoid, it is converted to CO<sub>2</sub> near  
 2 Rubisco by the carbonic anhydrase CAH3. In *Chlamydomonas*, CAH3 is positioned within  
 3 the thylakoid-derived “pyrenoid tubules” that traverse the Rubisco matrix, providing a  
 4 membrane-associated site for HCO<sub>3</sub><sup>-</sup> to CO<sub>2</sub> conversion adjacent to the condensate  
 5 (Mackinder et al., 2017; Hennacy and Jonikas, 2020). However, traversing membranes are  
 6 not universal across pyrenoids: while many algal pyrenoids are penetrated by thylakoid  
 7 tubules or sheets, others show a homogeneous matrix that is not traversed by thylakoids,  
 8 indicating that different lineages can achieve pyrenoid function with distinct internal  
 9 membrane architectures (Kowallik, 1969; Stoyneva et al., 2009; Gärtner et al., 2012;  
 10 Herburger et al., 2016).

11           In *A. agrestis*, the architecture is explicitly non-traversing and CAH3 is not  
 12 concentrated in matrix-penetrating tubules. Instead, it is enriched in thylakoids in the  
 13 central chloroplast space, around which multiple pyrenoids are organized (Fig. 3). CAH3  
 14 signals form puncta that are concentrated adjacent to the interior-facing side of pyrenoids  
 15 (Robison et al., 2025; Ruaud et al., 2025). The thylakoid HCO<sub>3</sub><sup>-</sup> channel BST1 is distributed  
 16 across the thylakoid network but shows elevated signal on thylakoids immediately  
 17 adjacent to pyrenoids (Robison et al., 2025), consistent with localized delivery of HCO<sub>3</sub><sup>-</sup> to  
 18 the lumen near pyrenoids. Thus, pyrenoids can couple luminal CO<sub>2</sub> generation to Rubisco  
 19 using either (i) intrapyrenoid tubules within a more continuous matrix (e.g.,  
 20 *Chlamydomonas*) or (ii) distributed thylakoid contacts around multiple pyrenoid units (e.g.,  
 21 *A. agrestis*). Hornwort pyrenoid diversity includes more *Chlamydomonas*-like  
 22 organizational endpoints (e.g., *Notothylas*), suggesting a continuum of solutions for  
 23 positioning CCM transport modules relative to the condensate.

24

## 25 **CO<sub>2</sub> recapture**

26 Pyrenoids are also accompanied by a CO<sub>2</sub> recapture system to minimize loss of CO<sub>2</sub> that  
 27 leaks from the Rubisco-rich matrix. In *Chlamydomonas*, the CA-like protein LCIB  
 28 accumulates at the pyrenoid periphery under very low CO<sub>2</sub> (i.e., sub-ambient CO<sub>2</sub> levels;  
 29 Toyokawa et al., 2020), where it is positioned to rehydrate leaked CO<sub>2</sub> back to HCO<sub>3</sub><sup>-</sup> (often  
 30 described as localizing around gaps in the starch sheath), effectively acting as a  
 31 “peripheral CO<sub>2</sub> trap.” In *A. agrestis*, by contrast, fluorescently tagged LCIB does not  
 32 concentrate around individual pyrenoids and instead localizes to the chloroplast envelope,  
 33 co-localizing with an inner chloroplast envelope marker (Fig. 3) (Robison et al., 2025;  
 34 Ruaud et al., 2025). This envelope localization is functionally logical because hornwort  
 35 CAH3 is enriched outside the pyrenoid matrix (in the inter-pyrenoid thylakoid network),  
 36 placing LCIB around each pyrenoid could “steal” CO<sub>2</sub> immediately after it is generated,

1 short-circuiting the CCM. Consistent with reaction-diffusion modelling for thylakoid-  
 2 encased pyrenoids (Fei et al., 2022), LCIB positioned at the envelope is predicted to be  
 3 optimal: far enough away to avoid intercepting CO<sub>2</sub> near Rubisco, but still able to serve as a  
 4 “last line of defense” for CO<sub>2</sub> leakage. Finally, envelope-localized LCIB could also rapidly  
 5 convert any CO<sub>2</sub> that diffuses into the chloroplast into HCO<sub>3</sub><sup>-</sup> before it diffuses back out,  
 6 potentially supporting a partially “passive” mode of CO<sub>2</sub> chloroplast entry in *A. agrestis*.

7

8

### 9 **No starch sheath, no problem?**

10 In many green algae, the pyrenoid matrix is surrounded by a starch sheath that is induced  
 11 or enhanced under CCM conditions and is thought to reduce CO<sub>2</sub> leakage from the  
 12 Rubisco-rich condensate, although there is no direct evidence for this role (Itakura et al.,  
 13 2019; Toyokawa et al., 2020; Fei et al., 2022). While, the starch sheath is important for CCM  
 14 efficiency in *Chlamydomonas* (Adler et al., 2025), it is difficult to disentangle the diffusion  
 15 barrier hypothesis from its organizational role in the CCM. Beyond acting as a diffusion  
 16 barrier, the sheath also helps organize the peri-pyrenoid CO<sub>2</sub>-recapture system: in  
 17 *Chlamydomonas*, starch-sheath mutants mis-localize LCIB and show impaired CCM  
 18 function, consistent with the sheath providing spatial cues/scaffolding for recapture  
 19 around the matrix (Toyokawa et al., 2020).

20 While many green algal pyrenoids are surrounded by starch plates, starch sheaths  
 21 are not universal: diatom and hornwort pyrenoids lack a starch sheath, but may employ  
 22 alternative boundary layers. For example, a proteinaceous casing in diatoms (Shimakawa  
 23 et al., 2024), non-starch polysaccharide deposits in *Micromonas pusilla* (van Baren et al.  
 24 2016), or multiple stacked thylakoid layers that encase the pyrenoid matrix in hornworts.  
 25 “Naked” pyrenoids that lack a discernable boundary layer have also been observed in  
 26 *Porphyridium purpureum* (*Porphyridium cruentum* in the study; (Brody and Vatter, 1959)).  
 27 Together, these examples highlight that different lineages can evolve distinct diffusion-  
 28 barrier architectures to support the same core CCM objective: retaining elevated CO<sub>2</sub> in the  
 29 vicinity of Rubisco.

30

31 Engineering opportunities

32 Multiple modeling studies suggest that elevating CO<sub>2</sub> around Rubisco via a biophysical  
 33 CCM could substantially increase photosynthetic performance in C<sub>3</sub> crops (Long et al.,  
 34 2025). For example, modelling suggests that introducing a cyanobacterial-style CCM into  
 35 C<sub>3</sub> leaves could increase CO<sub>2</sub> uptake by ~60%, and, by analogy to yield responses observed

1 under elevated-CO<sub>2</sub> field conditions, this magnitude of improvement could plausibly  
2 translate to ~36–60% yield increases under appropriate constraints (McGrath and Long,  
3 2014; Atkinson et al., 2016). More recently, detailed reaction-diffusion and energetic pCCM  
4 modeling has provided an explicit engineering roadmap for pyrenoid-based CCMs, and  
5 predicted that appropriately configured architecture could markedly boost chloroplast CO<sub>2</sub>  
6 fixation (Fei et al., 2022).

7 Proto-pyrenoids, which we define as condensates comprising Rubisco and a linker  
8 protein, have been successfully assembled in C3 plant chloroplasts. Such condensates  
9 have been induced using EPYC1 in *Arabidopsis thaliana* (Atkinson et al., 2020), and by  
10 expressing RbcS-STAR in both *Anthoceros fusiformis* (a pyrenoid-absent hornwort species)  
11 and *Arabidopsis* (Robison et al., 2026). However, an efficient and functional pyrenoid  
12 requires “plumbing” to/from Rubisco within the pyrenoid matrix. This involves thylakoid-  
13 associated bicarbonate transport, CO<sub>2</sub> generation near the pyrenoid matrix, and (likely)  
14 diffusion-barrier architecture. Mechanistic work in *Chlamydomonas* has identified proteins  
15 that organize key architectural features of the native pyrenoid, including matrix-starch  
16 sheath organization and specialized pyrenoid-associated membrane structure formation  
17 (Itakura et al., 2019; Hennacy et al., 2024). In a plant-engineering context, expressing  
18 additional algal components has begun to push proto-pyrenoids toward more pyrenoid-like  
19 architecture and functionality. For example, SAGA1 and SAGA2 are two pyrenoid-  
20 associated proteins with motifs that bind both Rubisco and starch, effectively connecting  
21 the Rubisco matrix to the starch sheath. Introducing SAGA1/SAGA2 into *Arabidopsis* drives  
22 the formation of starch plate-like structures around engineered proto-pyrenoids (Atkinson  
23 et al., 2024).

24 In parallel to algal-to-crop transplantation efforts, hornworts provide an appealing  
25 second blueprint because they are the only embryophytes with pyrenoids, meaning their  
26 condensates operate inside a land-plant cellular and plastid environment (Villarreal and  
27 Renner, 2012). This matters because a pCCM is not just a Rubisco droplet: performance  
28 depends on the spatial organization and choreography of membranes, lumenal pH  
29 gradients, carbonic anhydrase localization, and diffusion barriers relative to the Rubisco-  
30 rich matrix. Hornwort pyrenoids exhibit diverse ultrastructures, and many species show  
31 strong integration of the Rubisco matrix with land-plant-like thylakoid architecture  
32 (including grana/lamellae), highlighting that a “land-plant chassis” can support pyrenoid  
33 operation. Our recent *A. agrestis* spatial model sharpens this engineering appeal: rather  
34 than relying on a *Chlamydomonas*-like traversing pyrenoid tubule system, a hornwort  
35 “land-plant pyrenoid chassis” may reduce some of the architectural mismatch that could  
36 arise when transferring algal systems wholesale into crops.

1 A particularly attractive hornwort feature is the innate Rubisco linker. Where EPYC1-,  
2 PYCO1-, and CsLinker-driven condensation depends on specific Rubisco subunit  
3 interaction surfaces (and thus typically requires installing algal Rubisco sequence-  
4 structure), RbcS-STAR self-associates. As mentioned earlier, expressing RbcS-STAR in  
5 *Arabidopsis* is sufficient to induce Rubisco condensates. Appending just the STAR domain  
6 from RbcS-STAR to *Arabidopsis* RbcS was also sufficient for proto-pyrenoid formation in  
7 *Arabidopsis* chloroplasts (Robison et al., 2026). Thus, RbcS-STAR represents a truly  
8 Rubisco-agnostic linker system that requires no modification of the host Rubisco  
9 structure-function.

10 A pragmatic path forward may be a modular, and explicitly hybrid, engineering  
11 strategy: leveraging hornwort-derived components for embryophyte chloroplast  
12 environment compatibility, while importing algal parts where they provide uniquely well-  
13 resolved functions. In practice, this could mean driving condensation with the *A. agrestis*  
14 STAR linker, which can drive proto-pyrenoid formation without requiring modification of  
15 native crop Rubisco, and then layering in *Chlamydomonas* bicarbonate delivery modules  
16 as needed. For example, thylakoid-coupled bicarbonate delivery and luminal CO<sub>2</sub>-  
17 generation concepts that have strong mechanistic and modeling support (Fei et al., 2022),  
18 along with additional algal components that fine-tune boundary conditions (e.g., starch-  
19 associated organization factors), where beneficial. Framed this way, hornwort pyrenoids  
20 are not a replacement for *Chlamydomonas*-inspired engineering, but a more directly  
21 translatable foundation for crops that can be strengthened by selectively importing algal  
22 parts with clear, modular functionality.

## 23 24 Conclusions

25 As the only land plants that possess a pCCM, hornworts provide not only critical insights  
26 into the evolution of pyrenoids but also key components for engineering pCCMs in crop  
27 plants. Recent studies leveraging the emerging model species *A. agrestis* have revealed a  
28 CO<sub>2</sub>-concentrating chassis broadly similar to that of *Chlamydomonas*. However, *A.*  
29 *agrestis* employs a drastically different strategy to condense Rubisco, relying on the innate,  
30 self-associating linker RbcS-STAR. Together, these features position hornworts as a  
31 uniquely tractable bridge between algal and terrestrial pCCMs.

## 32 Acknowledgements

33 We thank Silvia Pressel and Jeff Duckett for kindly sharing their SEM image (Figure 1D) and  
34 Karen S. Renzaglia for sharing TEM micrographs (Fig 2).

## 1 Funding

2 L.H.G. acknowledges funding from the Hypothesis Fund, the U.S. Department of Energy  
3 (grant no. DE-SC0024175), and National Science Foundation (MCB-2213840). F-W.L  
4 acknowledges funding from the National Science Foundation (MCB-2213841). J.C.V.A  
5 acknowledges funding from Canada Research Chair 950–232698.

## 6 Author contributions

7 All authors contributed equally to the conception and scope of the article, literature review  
8 and synthesis, writing of the manuscript, preparation of figures, and final editing. All  
9 authors approved the final submitted version.

## 10 Conflict of Interest statement

11 The authors have no conflicts to declare.

ACCEPTED MANUSCRIPT

## 1 Box 1. Recent advances in hornwort pyrenoid biology

- 2 ● The emergence of *Anthoceros agrestis* as a tractable land-plant pyrenoid model  
3 system has enabled routine live imaging, localization studies, and genetic  
4 manipulation of pCCM components.
- 5 ● Hornwort pCCMs use a spatial architecture distinct from *Chlamydomonas*, with  
6 different organization and placement of membranes and CO<sub>2</sub>-delivery systems.
- 7 ● Hornwort pyrenoid condensation can be driven by an ‘innate’ Rubisco linker (RbcS-  
8 STAR), in which Rubisco-incorporated STAR extensions self-associate.
- 9 ● Independent pyrenoid origins in hornworts are accompanied by distinct linker  
10 solutions, highlighting convergent routes to Rubisco condensation.
- 11 ● Hornwort Rubisco has unconventional assembly-factor dependencies and kinetic  
12 behaviors compared with canonical land-plant Rubisco, expanding the known  
13 landscape of Rubisco biogenesis and structure-function relationships.
- 14 ● Proto-pyrenoids have been assembled in C<sub>3</sub> plant chloroplasts using algal and  
15 hornwort linkers.
- 16 ● Hornwort pyrenoids provide a land-plant chassis for hybrid pCCM engineering.  
17

## 18 Box 2. Outstanding Questions

- 19 ● How does inorganic carbon enter hornwort chloroplasts, and what are the  
20 chloroplast-envelope Ci transporters that replace the role of LCIA in lineages  
21 lacking a clear LCIA ortholog?
- 22 ● Where do core pCCM components (e.g., CAH3, BST1, and LCIB) localize in  
23 pyrenoid-absent hornwort species?
- 24 ● What diversity of linker mechanisms exist in hornwort species?
- 25 ● What is the functional role of channel thylakoids in hornwort photosynthesis?
- 26 ● Are hornwort pCCMs truly constitutive, or are they environmentally tunable across  
27 CO<sub>2</sub>, hydration state, light, and/or development?
- 28 ● What are the energetic costs of operating hornwort pyrenoids, and how are these  
29 balanced?
- 30 ● What is the minimal module set required to achieve a functional pyrenoid CCM in  
31 crop chloroplasts?  
32  
33  
34  
35

## 1 References

- 2 **Adler L, Lau J, Esch L, Dao O, Barrett J, Grant S, Yates G, McCormick AJ, Mackinder LCM**  
3 (2025) LCI9 is required for normal pyrenoid starch sheath formation and efficiency of  
4 the CO<sub>2</sub>-concentrating mechanism in *Chlamydomonas reinhardtii*. bioRxiv 2025.11.  
5 18.689020
- 6 **Aigner H, Wilson RH, Bracher A, Calisse L, Bhat JY, Hartl FU, Hayer-Hartl M** (2017) Plant  
7 RuBisCo assembly in *E. coli* with five chloroplast chaperones including BSD2. *Science*  
8 **358**: 1272–1278
- 9 **Atkinson N, Feike D, Mackinder LCM, Meyer MT, Griffiths H, Jonikas MC, Smith AM,**  
10 **McCormick AJ** (2016) Introducing an algal carbon-concentrating mechanism into  
11 higher plants: location and incorporation of key components. *Plant Biotechnol J* **14**:  
12 1302–1315
- 13 **Atkinson N, Mao Y, Chan KX, McCormick AJ** (2020) Condensation of Rubisco into a proto-  
14 pyrenoid in higher plant chloroplasts. *Nat Commun* **11**: 6303
- 15 **Atkinson N, Stringer R, Mitchell SR, Seung D, McCormick AJ** (2024) SAGA1 and SAGA2  
16 promote starch formation around proto-pyrenoids in *Arabidopsis* chloroplasts. *Proc*  
17 *Natl Acad Sci U S A* **121**: e2311013121
- 18 **Badger MR, Price GD** (1992) The CO<sub>2</sub> concentrating mechanism in cyanobacteria and  
19 microalgae. *Physiol Plant* **84**: 606–615
- 20 **Barrett J, Naduthodi MIS, Mao Y, Dégut C, Musiał S, Salter A, Leake MC, Plevin MJ,**  
21 **McCormick AJ, Blaza JN, et al** (2024) A promiscuous mechanism to phase separate  
22 eukaryotic carbon fixation in the green lineage. *Nat Plants* **10**: 1801–1813
- 23 **Barrett J, Nam O, Naduthodi MIS, Mackinder LCM** (2026) Pyrenoid structure, function,  
24 evolution, and characterization across diverse lineages. *Annu Rev Plant Biol*. doi:  
25 [10.1146/annurev-arplant-070225-034846](https://doi.org/10.1146/annurev-arplant-070225-034846)
- 26 **Bouvier JW, Emms DM, Rhodes T, Bolton JS, Brasnett A, Eddershaw A, Nielsen JR, Unitt**  
27 **A, Whitney SM, Kelly S** (2021) Rubisco Adaptation Is More Limited by Phylogenetic  
28 Constraint Than by Catalytic Trade-off. *Mol Biol Evol* **38**: 2880–2896
- 29 **Brody M, Vatter AE** (1959) Observations on cellular structures of *Porphyridium cruentum*. *J*  
30 *Biophys Biochem Cytol* **5**: 289–294
- 31 **Brown RM, Arnott HJ** (1970) Structure and function of the algal pyrenoid. I. Ultrastructure  
32 and cytochemistry during zoosporegenesis of *Tetracystis excentrica*1. *J Phycol* **6**: 14–  
33 22
- 34 **Burlacot A, Dao O, Auroy P, Cuiné S, Li-Beisson Y, Peltier G** (2022) Alternative

- 1 photosynthesis pathways drive the algal CO<sub>2</sub>-concentrating mechanism. *Nature* **605**:  
2 366–371
- 3 **Burr FA** (1970) Phylogenetic transitions in the chloroplasts of the Anthocerotales. I. The  
4 number and ultrastructure of the mature plastids. *Am J Bot* 97–110
- 5 **Busch FA** (2020) Photorespiration in the context of Rubisco biochemistry, CO<sub>2</sub> diffusion  
6 and metabolism. *Plant J* **101**: 919–939
- 7 **Clark JW, Harris BJ, Hetherington AJ, Hurtado-Castano N, Brench RA, Casson S,**  
8 **Williams TA, Gray JE, Hetherington AM** (2022) The origin and evolution of stomata.  
9 *Curr Biol* **32**: R539–R553
- 10 **Emms DM, Covshoff S, Hibberd JM, Kelly S** (2016) Independent and parallel evolution of  
11 new genes by gene duplication in two origins of C<sub>4</sub> photosynthesis provides new  
12 insight into the mechanism of phloem loading in C<sub>4</sub> species. *Mol Biol Evol* **33**: 1796–  
13 1806
- 14 **Fei C, Wilson AT, Mangan NM, Wingreen NS, Jonikas MC** (2022) Modelling the pyrenoid-  
15 based CO<sub>2</sub>-concentrating mechanism provides insights into its operating principles  
16 and a roadmap for its engineering into crops. *Nat Plants* **8**: 583–595
- 17 **Flexas J, Clemente-Moreno MJ, Bota J, Brodribb TJ, Gago J, Mizokami Y, Nadal M,**  
18 **Perera-Castro AV, Roig-Oliver M, Sugiura D, et al** (2021) Cell wall thickness and  
19 composition are involved in photosynthetic limitation. *J Exp Bot* **72**: 3971–3986
- 20 **Fortin JP, Friedman WE** (2024) A stomate by any other name? The open question of  
21 hornwort gametophytic pores, their homology, and implications for the evolution of  
22 stomates. *New Phytol.* doi: [10.1111/nph.20094](https://doi.org/10.1111/nph.20094)
- 23 **Frangedakis E, Shimamura M, Villarreal JC, Li F-W, Tomaselli M, Waller M, Sakakibara**  
24 **K, Renzaglia KS, Szövényi P** (2021) The hornworts: morphology, evolution and  
25 development. *New Phytol* **229**: 735–754
- 26 **Freeman Rosenzweig ES, Xu B, Kuhn Cuellar L, Martinez-Sanchez A, Schaffer M,**  
27 **Strauss M, Cartwright HN, Ronceray P, Plitzko JM, Förster F, et al** (2017) The  
28 eukaryotic CO<sub>2</sub>-concentrating organelle is liquid-like and exhibits dynamic  
29 reorganization. *Cell* **171**: 148–162.e19
- 30 **Gärtner G, Stoyneva MP, Uzunov BA, Mancheva AD, Ingolić E** (2012) Ultrastructure of  
31 vegetative cells and autospores of an aerophytic strain of *Vischeria stellata* (Chodat ex  
32 Poulton) Pascher (Eustigmatophyceae) from Bulgaria. *Fottea (Praha)* **12**: 273–280
- 33 **Graham L, Lewis LA, Taylor W, Wellman C, Cook M** (2014) Early terrestrialization:  
34 Transition from algal to bryophyte grade. *Advances in Photosynthesis and Respiration.*  
35 Springer Netherlands, Dordrecht, pp 9–28

- 1 **Hagemann M, Bauwe H** (2016) Photorespiration and the potential to improve  
2 photosynthesis. *Curr Opin Chem Biol* **35**: 109–116
- 3 **Hanson DT, Andrews TJ, Badger MR** (2002) Variability of the pyrenoid-based CO<sub>2</sub>  
4 concentrating mechanism in hornworts (Anthocerotophyta). *Funct Plant Biol* **29**: 407–  
5 416
- 6 **Hanson DT, Renzaglia K, Villarreal JC** (2014) Diffusion Limitation and CO<sub>2</sub> Concentrating  
7 Mechanisms in Bryophytes. *In* DT Hanson, SK Rice, eds, *Photosynthesis in Bryophytes*  
8 *and Early Land Plants*. Springer Netherlands, Dordrecht, pp 95–111
- 9 **Hennacy JH, Atkinson N, Kayser-Browne A, Ergun SL, Franklin E, Wang L, Eicke S,**  
10 **Kazachkova Y, Kafri M, Fauser F, et al** (2024) SAGA1 and MITH1 produce matrix-  
11 traversing membranes in the CO<sub>2</sub>-fixing pyrenoid. *Nat Plants* **10**: 2038–2051
- 12 **Hennacy JH, Jonikas MC** (2020) Prospects for Engineering Biophysical CO<sub>2</sub> Concentrating  
13 Mechanisms into Land Plants to Enhance Yields. *Annu Rev Plant Biol* **71**: 461–485
- 14 **Herburger K, Karsten U, Holzinger A** (2016) *Entransia* and *Hormidiella*, sister lineages of  
15 *Klebsormidium* (Streptophyta), respond differently to light, temperature, and  
16 desiccation stress. *Protoplasma* **253**: 1309–1323
- 17 **Herfort L, Thake B, Roberts J** (2002) Acquisition and use of bicarbonate by *Emiliania*  
18 *huxleyi*. *New Phytol* **156**: 427–436
- 19 **He S, Chou H-T, Matthies D, Wunder T, Meyer MT, Atkinson N, Martinez-Sanchez A,**  
20 **Jeffrey PD, Port SA, Patena W, et al** (2020) The structural basis of Rubisco phase  
21 separation in the pyrenoid. *Nat Plants* **6**: 1480–1490
- 22 **He S, Crans VL, Jonikas MC** (2023) The pyrenoid: the eukaryotic CO<sub>2</sub>-concentrating  
23 organelle. *Plant Cell* **35**: 3236–3259
- 24 **He S, Lemma LM, Martinez-Calvo A, He G, Hennacy JH, Wang L, Ergun SL, Rai AK, Wang**  
25 **C, Bunday L, et al** (2025) Kinase KEY1 controls pyrenoid condensate size throughout  
26 the cell cycle by disrupting phase separation interactions. *bioRxiv* 2025.10.  
27 09.681382
- 28 **Hibberd JM, Covshoff S** (2010) The regulation of gene expression required for C<sub>4</sub>  
29 photosynthesis. *Annu Rev Plant Biol* **61**: 181–207
- 30 **Holdsworth RH** (1971) The isolation and partial characterization of the pyrenoid protein of  
31 *Eremosphaera viridis*. *J Cell Biol* **51**: 499–513
- 32 **Itakura AK, Chan KX, Atkinson N, Pallesen L, Wang L, Reeves G, Patena W, Caspari O,**  
33 **Roth R, Goodenough U, et al** (2019) A Rubisco-binding protein is required for normal  
34 pyrenoid number and starch sheath morphology in *Chlamydomonas reinhardtii*. *Proc*  
35 *Natl Acad Sci U S A* **116**: 18445–18454

- 1 **Kaja H** (1954) Untersuchungen über die Chromatophoren und Pyrenoide der  
2 Anthocerotales. *Protoplasma* **44**: 136–153
- 3 **Kikutani S, Nakajima K, Nagasato C, Tsuji Y, Miyatake A, Matsuda Y** (2016) Thylakoid  
4 luminal  $\theta$ -carbonic anhydrase critical for growth and photosynthesis in the marine  
5 diatom *Phaeodactylum tricornutum*. *Proc Natl Acad Sci U S A* **113**: 9828–9833
- 6 **Kowallik K** (1969) The crystal lattice of the pyrenoid matrix of *Prorocentrum micans*. *J Cell*  
7 *Sci* **5**: 251–269
- 8 **Küffner AM, Pommerenke B, Kley L, Ng JZY, Prinz S, Tinzl-Zechner M, Claus P, Paczia N,**  
9 **Zarzycki J, Hochberg GKA, et al** (2024) Bottom-up reconstruction of minimal  
10 pyrenoids provides insights into the evolution and mechanisms of carbon  
11 concentration by EPYC1 proteins. *bioRxiv*. doi: [10.1101/2024.06.28.601168](https://doi.org/10.1101/2024.06.28.601168)
- 12 **Lacoste-Royal G, Gibbs SP** (1987) Immunocytochemical localization of ribulose-1,5-  
13 biphosphate carboxylase in the pyrenoid and thylakoid region of the chloroplast of  
14 *Chlamydomonas reinhardtii*. *Plant Physiol* **83**: 602–606
- 15 **Lafferty DJ, Robison TA, Gunadi A, Schafran PW, Gunn LH, Van Eck J, Li F-W** (2024)  
16 Biolistics-mediated transformation of hornworts and its application to study pyrenoid  
17 protein localization. *J Exp Bot*. doi: [10.1093/jxb/erae243](https://doi.org/10.1093/jxb/erae243)
- 18 **Leggat W, Badger MR, Yellowlees D** (1999) Evidence for an inorganic carbon-  
19 concentrating mechanism in the symbiotic dinoflagellate *Symbiodinium* sp. *Plant*  
20 *Physiol* **121**: 1247–1256
- 21 **Li F-W, Nishiyama T, Waller M, Frangedakis E, Keller J, Li Z, Fernandez-Pozo N, Barker**  
22 **MS, Bennett T, Blázquez MA, et al** (2020) Anthoceros genomes illuminate the origin of  
23 land plants and the unique biology of hornworts. *Nat Plants* **6**: 259–272
- 24 **Li F-W, Villarreal Aguilar JC, Szövényi P** (2017) Hornworts: An overlooked window into  
25 carbon-concentrating mechanisms. *Trends Plant Sci* **22**: 275–277
- 26 **Liu L-N** (2022) Advances in the bacterial organelles for CO<sub>2</sub> fixation. *Trends Microbiol* **30**:  
27 567–580
- 28 **Loh DH, Gunn LH** (2025) A SynBio explosion: a whole new world for Rubisco engineering. *J*  
29 *Exp Bot* **76**: 2593–2597
- 30 **Long SP, Wang Y, Carmo-Silva E, Cavanagh AP, Jonikas MC, Kromdijk J, Long BM,**  
31 **Marshall-Colón A, Shukla D, Wilson RH, et al** (2025) Feeding from the sun-  
32 Successes and prospects in bioengineering photosynthesis for food security. *Cell* **188**:  
33 6700–6719
- 34 **Mackinder LCM, Chen C, Leib RD, Patena W, Blum SR, Rodman M, Ramundo S, Adams**  
35 **CM, Jonikas MC** (2017) A Spatial Interactome Reveals the Protein Organization of the

- 1 Algal CO<sub>2</sub>-Concentrating Mechanism. *Cell* **171**: 133–147.e14
- 2 **Mackinder LCM, Meyer MT, Mettler-Altman T, Chen VK, Mitchell MC, Caspari O,**  
3 **Freeman Rosenzweig ES, Pallesen L, Reeves G, Itakura A, et al** (2016) A repeat  
4 protein links Rubisco to form the eukaryotic carbon-concentrating organelle. *Proc Natl*  
5 *Acad Sci U S A* **113**: 5958–5963
- 6 **MacLeod AI, Raval PK, Stockhorst S, Knopp MR, Frangedakis E, Gould SB** (2022) Loss of  
7 Plastid developmental genes coincides with a reversion to monoplastidy in hornworts.  
8 *Front Plant Sci* **13**: 863076
- 9 **Manton I** (1962) Observations on Plastid Development in the Meristem of *Anthoceros*. *J Exp*  
10 *Bot* **13**: 325–326
- 11 **McAllister F** (1914) The pyrenoid of *Anthoceros*. *Am J Bot* **1**: 79–95
- 12 **McAllister F** (1927) The Pyrenoids of *Anthoceros* and *Notothydas* with Especial Reference  
13 to Their Presence in Spore Mother Cells. *Am J Bot* **14**: 246
- 14 **McGrath JM, Long SP** (2014) Can the Cyanobacterial Carbon-Concentrating Mechanism  
15 Increase Photosynthesis in Crop Species? A Theoretical Analysis. *Plant Physiol* **164**:  
16 2247–2261
- 17 **McKay RML, Gibbs SP** (1989) Immunocytochemical localization of ribulose 1,5-  
18 biphosphate carboxylase/oxygenase in light-limited and light-saturated cells  
19 of *Chlorella pyrenoidosa*. *Protoplasma* **149**: 31–37
- 20 **Menke W** (1961) Über die Chloroplasten von *Anthoceros punctatus*. *Z Naturforsch B J*  
21 *Chem Sci* **16**: 334–336
- 22 **Meyer MT, Griffiths H** (2013) Origins and diversity of eukaryotic CO<sub>2</sub>-concentrating  
23 mechanisms: lessons for the future. *J Exp Bot* **64**: 769–786
- 24 **Meyer MT, Seibt U, Griffiths H** (2008) To concentrate or ventilate? Carbon acquisition,  
25 isotope discrimination and physiological ecology of early land plant life forms. *Philos*  
26 *Trans R Soc Lond B Biol Sci* **363**: 2767–2778
- 27 **Meyer MT, Whittaker C, Griffiths H** (2017) The algal pyrenoid: key unanswered questions. *J*  
28 *Exp Bot* **68**: 3739–3749
- 29 **Moromizato R, Fukuda K, Suzuki S, Motomura T, Nagasato C, Hirakawa Y** (2024)  
30 Pyrenoid proteomics reveals independent evolution of the CO<sub>2</sub>-concentrating  
31 organelle in chlorarachniophytes. *Proc Natl Acad Sci U S A* **121**: e2318542121
- 32 **Morris JL, Puttick MN, Clark JW, Edwards D, Kenrick P, Pressel S, Wellman CH, Yang Z,**  
33 **Schneider H, Donoghue PCJ** (2018) The timescale of early land plant evolution. *Proc*  
34 *Natl Acad Sci U S A* **115**: E2274–E2283

- 1 **Nakajima K, Tanaka A, Matsuda Y** (2013) SLC4 family transporters in a marine diatom  
2 directly pump bicarbonate from seawater. *Proc Natl Acad Sci U S A* **110**: 1767–1772
- 3 **Nam O, Musiał S, Demulder M, McKenzie C, Dowle A, Dowson M, Barrett J, Blaza JN,**  
4 **Engel BD, Mackinder LCM** (2024) A protein blueprint of the diatom CO<sub>2</sub>-fixing  
5 organelle. *Cell* **187**: 5935–5950.e18
- 6 **Neofotis P, Temple J, Tessmer OL, Bibik J, Norris N, Pollner E, Lucker B, Weraduwage**  
7 **SM, Withrow A, Sears B, et al** (2021) The induction of pyrenoid synthesis by hyperoxia  
8 and its implications for the natural diversity of photosynthetic responses in  
9 *Chlamydomonas*. *Elife*. doi: [10.7554/eLife.67565](https://doi.org/10.7554/eLife.67565)
- 10 **Nimer NA, Merrett MJ** (1996) The development of a CO<sub>2</sub>-concentrating mechanism in  
11 *Emiliana huxleyi*. *New Phytol* **133**: 383–389
- 12 **Nishiyama T, Wolf PG, Kugita M, Sinclair RB, Sugita M, Sugiura C, Wakasugi T, Yamada**  
13 **K, Yoshinaga K, Yamaguchi K, et al** (2004) Chloroplast phylogeny indicates that  
14 bryophytes are monophyletic. *Mol Biol Evol* **21**: 1813–1819
- 15 **Oh ZG, Ang WSL, Poh CW, Lai S-K, Sze SK, Li H-Y, Bhushan S, Wunder T, Mueller-Cajar**  
16 **O** (2023) A linker protein from a red-type pyrenoid phase separates with Rubisco via  
17 oligomerizing sticker motifs. *Proc Natl Acad Sci U S A* **120**: e2304833120
- 18 **Oh ZG, Robison TA, Loh DH, Ang WSL, Ng JZY, Li F-W, Gunn LH** (2024) Unique biogenesis  
19 and kinetics of hornwort Rubiscos revealed by synthetic biology systems. *Mol Plant* **17**:  
20 1833–1849
- 21 **One Thousand Plant Transcriptomes Initiative** (2019) One thousand plant  
22 transcriptomes and the phylogenomics of green plants. *Nature* **574**: 679–685
- 23 **Pellegrini M** (1980) Three-dimensional reconstruction of organelles in *Euglena gracilis* Z. I.  
24 Qualitative and quantitative changes of chloroplasts and mitochondrial reticulum in  
25 synchronous photoautotrophic culture. *J Cell Sci* **43**: 137–166
- 26 **Peñaloza-Bojacá G, Burleigh JG, Maciel-Silva A, Cargill DC, Bell D, Sessa EB, McDaniel**  
27 **SF, Davis EC, Endara L, Salazar Allen N, et al** (2025) Ancient reticulation, incomplete  
28 lineage sorting and the evolution of the pyrenoid at the dawn of hornwort  
29 diversification. *Ann Bot* **135**: 1199–1214
- 30 **Proctor, MCF** (2000) Physiological Ecology. *Bryophyte Biology* 1:225-247.
- 31
- 32 **Prywes N, Phillips NR, Tuck OT, Valentin-Alvarado LE, Savage DF** (2023) Rubisco  
33 function, evolution, and engineering. *Annu Rev Biochem* **92**: 385–410
- 34 **Raven JA, Giordano M** (2017) Acquisition and metabolism of carbon in the Ochrophyta

- 1 other than diatoms. *Philos Trans R Soc Lond B Biol Sci* **372**: 20160400
- 2 **Raven JA, Suggett DJ, Giordano M** (2020) Inorganic carbon concentrating mechanisms in  
3 free-living and symbiotic dinoflagellates and chromerids. *J Phycol* **56**: 1377–1397
- 4 **Renzaglia KS** (1978) Comparative morphology and developmental anatomy of the  
5 *Anthocerotophyta*. *J Hattori Bot Lab* **44**: 31–90
- 6 **Renzaglia KS, Villarreal Aguilar JC, Piatkowski BT, Lucas JR, Merced A** (2017) Hornwort  
7 Stomata: Architecture and Fate Shared with 400-Million-Year-Old Fossil Plants without  
8 Leaves. *Plant Physiol* **174**: 788–797
- 9 **Renzaglia KS, Villarreal JC, Duff RJ** (2009) New insights into morphology, anatomy, and  
10 systematics of hornworts. *Bryophyte biology* **2**: 139–171
- 11 **Robison TA, Mao Y, Oh ZG, Ang WSL, Loh DH, Hsieh Y-H, Ceminsky M, Atkinson N,**  
12 **Lafferty D, Xu X, et al** (2026) An unconventional Rubisco Small Subunit underpins the  
13 CO<sub>2</sub>-concentrating organelle in land plants. *Science* in press:
- 14 **Robison TA, Oh ZG, Lafferty D, Xu X, Villarreal JCA, Gunn LH, Li F-W** (2025) Hornworts  
15 reveal a spatial model for pyrenoid-based CO<sub>2</sub>-concentrating mechanisms in land  
16 plants. *Nat Plants* 1–11
- 17 **Roig-Oliver M, Douthe C, Bota J, Flexas J** (2021) Cell wall thickness and composition are  
18 related to photosynthesis in Antarctic mosses. *Physiol Plant* **173**: 1914–1925
- 19 **Rousk K, Villarreal A JC** (2025) Time to end the vascular plant chauvinism. *Nat Plants* **11**: 3
- 20 **Ruaud S, Nötzold SI, Waller M, Galbier F, Mousavi SS, Charran M, Mateos JM, Zeeman**  
21 **S, Baily A, Baroux C, et al** (2025) Molecular underpinnings of hornwort CO<sub>2</sub>  
22 concentrating mechanisms: subcellular localization of putative key molecular  
23 components in the model hornwort *Anthoceros agrestis*. *New Phytologist*. doi:  
24 [10.1111/nph.70167](https://doi.org/10.1111/nph.70167)
- 25 **Sage RF** (2016) Photosynthesis: Mining grasses for a better Rubisco. *Nat Plants*. doi:  
26 [10.1038/nplants.2016.192](https://doi.org/10.1038/nplants.2016.192)
- 27 **Sage RF** (2002) Variation in the *k*(cat) of Rubisco in C(3) and C(4) plants and some  
28 implications for photosynthetic performance at high and low temperature. *J Exp Bot*  
29 **53**: 609–620
- 30 **Schafran P, Hauser DA, Nelson JM, Xu X, Mueller LA, Kulshrestha S, Smalley I, de Vries**  
31 **S, Irisarri I, de Vries J, et al** (2025) Pan-phylum genomes of hornworts reveal  
32 conserved autosomes but dynamic accessory and sex chromosomes. *Nat Plants* 1–14
- 33 **Scherrer A** (1914) Untersuchungen über Bau und Vermehrung der Chromatophoren und  
34 das Vorkommen von Chondriosomen bei *Anthoceros*. *Flora Oder Allg Bot Ztg* **107**: 1–

- 1 56.e11
- 2 **Shimakawa G, Demulder M, Flori S, Kawamoto A, Tsuji Y, Nawaly H, Tanaka A, Tohda R,**  
3 **Ota T, Matsui H, et al** (2024) Diatom pyrenoids are encased in a protein shell that  
4 enables efficient CO<sub>2</sub> fixation. *Cell* **187**: 5919–5934.e19
- 5 **Sinetova MA, Kupriyanova EV, Markelova AG, Allakhverdiev SI, Pronina NA** (2012)  
6 Identification and functional role of the carbonic anhydrase Cah3 in thylakoid  
7 membranes of pyrenoid of *Chlamydomonas reinhardtii*. *Biochim Biophys Acta* **1817**:  
8 1248–1255
- 9 **Smith EC, Griffiths H** (1996) A pyrenoid-based carbon-concentrating mechanism is  
10 present in terrestrial bryophytes of the class Anthocerotae. *Planta* **200**: 203–212
- 11 **Smith EC, Griffiths H** (2000) The role of carbonic anhydrase in photosynthesis and the  
12 activity of the carbon-concentrating-mechanism in bryophytes of the class  
13 Anthocerotae. *New Phytol* **145**: 29–37
- 14 **Söderström L, Hagborg A, von Konrat M, Bartholomew-Began S, Bell D, Briscoe L,**  
15 **Brown E, Cargill DC, Costa DP, Crandall-Stotler BJ, et al** (2016) World checklist of  
16 hornworts and liverworts. *PhytoKeys* **59**: 1–828
- 17 **Stoyneva MP, Ingolić E, Gärtner G, Vyverman W** (2009) The pyrenoid ultrastructure in  
18 *Oocystis lacustris*. *Fottea (Praha)* **9**: 149–154
- 19 **Sun CN** (1962) Submicroscopic structure and development of the chloroplast and  
20 pyrenoid in *Anthoceros laevis*. *Protoplasma* **55**: 89–98
- 21 **Tcherkez G, Farquhar GD** (2021) Rubisco catalytic adaptation is mostly driven by  
22 photosynthetic conditions - Not by phylogenetic constraints. *J Plant Physiol* **267**:  
23 153554
- 24 **Tholen D, Zhu X-G** (2011) The mechanistic basis of internal conductance: a theoretical  
25 analysis of mesophyll cell photosynthesis and CO<sub>2</sub> diffusion. *Plant Physiol* **156**: 90–  
26 105
- 27 **Toyokawa C, Yamano T, Fukuzawa H** (2020) Pyrenoid starch sheath is required for LCIB  
28 localization and the CO<sub>2</sub>-concentrating mechanism in green algae. *Plant Physiol* **182**:  
29 1883–1893
- 30 **Valentine LJ, Campbell EO, Hopcroft DH** (1986) A study of chloroplast structure in 3  
31 Megaceros species and 3 Dendroceros species (Anthocerotae) indigenous to New  
32 Zealand. *N Z J Bot* **24**: 1–8
- 33 **Vaughn KC, Campbell EO, Hasegawa J, Owen HA, Renzaglia KS** (1990) The pyrenoid is  
34 the site of ribulose 1,5-bisphosphate carboxylase/oxygenase accumulation in the  
35 hornwort (Bryophyta: Anthocerotae) chloroplast. *Protoplasma* **156**: 117–129

- 1 **Vaughn KC, Ligrone R, Owen HA, Hasegawa J, Campbell EO, Renzaglia KS, Monge**  
2 **Najera J** (1992) The anthocero chloroplast: a review. *New Phytol* **120**: 169–190
- 3 **Villarejo A, Orús MI, Ramazanov Z, Martínez F** (1998) A 38-kilodalton low-CO<sub>2</sub>-inducible  
4 polypeptide is associated with the pyrenoid in *Chlorella vulgaris*. *Planta* **206**: 416–425
- 5 **Villarreal Aguilar JC, Renzaglia KS** (2015) The hornworts: important advancements in  
6 early land plant evolution. *J Bryol* **37**: 157–170
- 7 **Villarreal JC, Renner SS** (2012) Hornwort pyrenoids, carbon-concentrating structures,  
8 evolved and were lost at least five times during the last 100 million years. *Proc Natl*  
9 *Acad Sci U S A* **109**: 18873–18878
- 10 **de Vries J, Archibald JM** (2018) Plant evolution: landmarks on the path to terrestrial life.  
11 *New Phytol* **217**: 1428–1434
- 12 **Walker BJ, VanLoocke A, Bernacchi CJ, Ort DR** (2016) The costs of photorespiration to  
13 food production now and in the future. *Annu Rev Plant Biol* **67**: 107–129
- 14 **Wang L, Jonikas MC** (2020) The pyrenoid. *Curr Biol* **30**: R456–R458
- 15 **Whitney SM, Houtz RL, Alonso H** (2011) Advancing our understanding and capacity to  
16 engineer nature's CO<sub>2</sub>-sequestering enzyme, Rubisco. *Plant Physiol* **155**: 27–35
- 17 **Wickett NJ, Mirarab S, Nguyen N, Warnow T, Carpenter E, Matasci N, Ayyampalayam S,**  
18 **Barker MS, Burleigh JG, Gitzendanner MA, et al** (2014) Phylotranscriptomic analysis  
19 of the origin and early diversification of land plants. *Proc Natl Acad Sci U S A* **111**:  
20 E4859–68
- 21 **Wilsenach R** (1963) Differentiation of the chloroplast of *Anthoceros*. *J Cell Biol* **18**: 419–  
22 428
- 23 **Wujek DE** (1966) The Fine Structure of the Pyrenoid of *Anthoceros punctatus*. *Trans Kans*  
24 *Acad Sci* **69**: 314
- 25 **Wunder T, Oh ZG, Mueller-Cajar O** (2019) CO<sub>2</sub>-fixing liquid droplets: Towards a dissection  
26 of the microalgal pyrenoid. *Traffic* **20**: 380–389
- 27 **Young JN, Hopkinson BM** (2017) The potential for co-evolution of CO<sub>2</sub>-concentrating  
28 mechanisms and Rubisco in diatoms. *J Exp Bot* **68**: 3751–3762
- 29
- 30

1 Figure Legends

2 Figure 1. **Hornworts are the only land plants with pyrenoids.** (A) Phylogeny of major plant  
 3 groups. Lineages that have pyrenoids are colored green. (B) A hornwort plant with  
 4 sporophytes (2n; arrowhead) and gametophytes (n; arrow) indicated. (C) The model  
 5 hornwort *Anthoceros agrestis* expressing GFP-tagged Rubisco activase (RCA; green), which  
 6 localizes to pyrenoids and therefore serves as a fluorescent marker for pyrenoid position  
 7 within chloroplasts (blue). Scale bar, 10  $\mu\text{m}$ . (D) Pseudocolored scanning electron  
 8 microscope image of a hornwort chloroplast (green), showing multiple pyrenoids (purple).  
 9 Scale bar, 5  $\mu\text{m}$ .

10

11 Figure 2. **Pyrenoid diversity.** (A) Simplified hornwort chronogram with mapped plastid (uni  
 12 or multiplastidic) and pyrenoid evolution. Pyrenoid-containing lineages and pyrenoid-  
 13 lacking lineages are colored red and blue, respectively. An asterisk (\*) indicates that some  
 14 species in the genus lack pyrenoids. (B) Depiction of intrinsically disordered linkers, which  
 15 have motifs (red circles) that bind to either the Rubisco large or small subunit. (C) Depiction  
 16 of RbcS-STAR, an innate linker which is integrated into Rubisco and binds to other linkers,  
 17 rather than Rubisco. Rubisco large subunits, canonical RbcS, and RbcS-STAR are shown in  
 18 dark gray, light gray, and different colors, respectively.

19

20 Figure 3. **A spatial model of the pCCM in hornworts.** This schematic summarizes a working  
 21 model for  $\text{C}_i$  fluxes and  $\text{CO}_2$  elevation around condensed Rubisco in *A. agrestis*.  $\text{C}_i$  is  
 22 predicted to enter the cytosol and chloroplast primarily as  $\text{CO}_2$ . BST1 at the thylakoid  
 23 membrane is hypothesized to mediate  $\text{HCO}_3^-$  entry into the thylakoid lumen. LCIB at the  
 24 chloroplast envelope is proposed to retain stromal  $\text{C}_i$  by trapping incoming  $\text{CO}_2$  and  
 25 recapturing  $\text{CO}_2$  that leaks from the pyrenoid region. CAH3 is enriched in specialized,  
 26 centrally positioned thylakoids associated with the pyrenoid and is hypothesized to generate  
 27  $\text{CO}_2$  near the matrix. The matrix is a phase-separated, Rubisco enriched compartment  
 28 (depicted in magenta), and the surrounding thylakoids are proposed to act as a diffusional  
 29 barrier. Possible bicarbonate import from the cytosol and into the chloroplast is depicted  
 30 with lower opacity vectors to indicate a lack of evidence. Dashed arrows indicate  $\text{CO}_2$   
 31 movement; solid arrows indicate  $\text{HCO}_3^-$  movement.  $\text{C}_i$ , inorganic carbon; LCIB, Low Carbon  
 32 Inducible protein B; CAH3, Carbonic Anhydrase 3; BST1, Bestrophin-like channel 1.

33

34